NASA TECHNICAL REPORT

NASA TR R-321

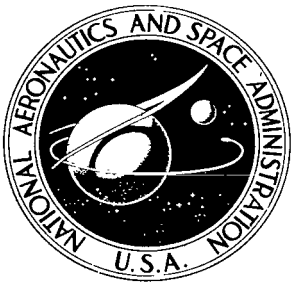

CALIBRATION OF PEGASUS AND EXPLORER XXIII DETECTOR PANELS

by Robert J. Naumann, David W. Jex, and Clyde L. Johnson

George C. Marshall Space Flight Center
Marshall, Ala.

NATIONAL AERONAUTICS AND SPACE ADMINISTRATION • WASHINGTON, D. C. • SEPTEMBER 1969

1. REPORT NO. NASA TR R-321	2. GOVERNMENT ACCESSION NO.	3. RECIPIENT'S CATALOG NO.
4. TITLE AND SUBTITLE Calibration of Pegasus and Explorer XXIII Detector Panels		5. REPORT DATE September 1969 6. PERFORMING ORGANIZATION CODE
7. AUTHOR(S) Robert J. Naumann, David W. Jex, and Clyde L. Johnson		8. PERFORMING ORGANIZATION REPORT # M430
9. PERFORMING ORGANIZATION NAME AND ADDRESS George C. Marshall Space Flight Center Marshall Space Flight Center, Alabama 35812		10. WORK UNIT NO. 11. CONTRACT OR GRANT NO.
12. SPONSORING AGENCY NAME AND ADDRESS		13. TYPE OF REPORT & PERIOD COVERED NASA Technical Report 14. SPONSORING AGENCY CODE

15. SUPPLEMENTARY NOTES

Work performed in Space Sciences Laboratory

16. ABSTRACT

Several series of tests were conducted to establish the ballistic limit for the various Pegasus and Explorer XXIII detector panels. In these tests extremely small, carefully sized beads were launched in a velocity range that included the perforation threshold. By varying the size, a ballistic limit curve was established on a mass-velocity plot. Such curves were then extrapolated to average meteor velocity to obtain the characteristic mass for each sensor.

Additional tests were conducted on the Pegasus panels using the Pegasus test tool, which contains the identical electronic circuitry used by the flight models. These tests included hot and cold tests, thermal cycling after impact, oblique impacts, etc. Several types of anomalous events noted in the operation of the spacecraft could be simulated in this manner. Some indication of the dependence of detection threshold upon size was obtained, and the implications of these tests in the analysis of the results will be discussed.

17. KEY WORDS	18. DISTRIBUTION STATEMENT		
19. SECURITY CLASSIF. (of this report) U	20. SECURITY CLASSIF. (of this page) U	21. NO. OF PAGES 37	22. PRICE * $3.00

*For sale by the Clearinghouse for Federal Scientific and Technical Information
Springfield, Virginia 22151

TABLE OF CONTENTS

LIST OF ILLUSTRATIONS

LIST OF TABLES

CALIBRATION OF PEGASUS AND EXPLORER XXIII DETECTOR PANELS

SUMMARY

Pegasus and Explorer XXIII detector panels were calibrated by determining the perforation velocity required for various laboratory masses. These results were extrapolated to average meteoroid velocity and density, taken to be 19.17 km/sec and 0.5 gm/cm^3, respectively, by requiring that $M^{0.352}\ \rho^{0.148}\ V^{0.875}$ remain constant. The threshold masses of meteoroids of average density impacting these sensors at normal incidence at average velocity were found to be

Detector	Mass (gm)
0.0406 (Pegasus)	9.6×10^{-7}
0.0226 (Pegasus)	2.3×10^{-7}
0.00508 (Explorer XXIII)	2.9×10^{-8}
0.00254 (Explorer XXIII)	7.7×10^{-9}

INTRODUCTION

The three Pegasus satellites and Explorers XVI and XXIII have measured the rate at which various materials are perforated by meteoroids in the vicinity of the earth. Such information is useful for assessing the hazard imposed by meteoroids, since the damage is measured directly. However, it is also desirable to relate such measurements to other properties of meteoroids, such as their mass distribution for comparison with other measurements. For this purpose, a series of tests has been conducted in various laboratories.

The object of these tests was to establish the threshold conditions under which the various sensors in question would respond. Since meteoroid velocities cannot yet be attained in the laboratory, it was necessary to establish the threshold conditions for several projectile sizes and velocities. In this manner, an extrapolation to the threshold mass at meteoroid velocity may be made.

EXPERIMENTAL PROCEDURE

Calibration was done by selecting a given sized projectile and launching it at various velocities until a critical velocity was established that just caused threshold damage. Threshold damage was taken as perforation of the primary target thickness so that light could pass through it. The pressurized cells on Explorer XVI and Explorer XXIII respond to any leak; therefore, it is reasonable to consider any particle that causes perforation allowing passage of light as having threshold or greater mass. For the capacitor-type detectors used on Pegasus, the situation becomes somewhat more complicated. It has been found in the laboratory that particles causing threshold perforation do not always produce detectable responses. The detection probability appears to increase for larger particles. Therefore, as for the Explorers, the mass causing threshold perforation will be sought, and the detection probability will be used to adjust the flux measurements.

One of the major difficulties in calibrating the flight detectors lies in the very small particle sizes that must be used. Particles as small as 20 microns were used for the thinnest detector samples. With such sizes, there is no method of photographing the projectile just prior to impact, as is standard procedure in most hyperballistic ranges. Even if such a particle could be resolved, at 10 km/sec it travels its own diameter in 2 nanoseconds, which makes it beyond the state of the art to stop its motion. In any launch process there is fine, high-velocity debris from gun parts, fragmented projectiles, sabot fragments, etc. In dealing with larger projectiles, the presence of such debris is not usually a problem since the damage from the projectile can obviously be distinguished from debris. However, when the projectile size is smaller than some of the debris, it becomes very difficult to make such a determination.

Most of the small projectile work in this program was performed by the Space and Information Division of North American Aviation (now North American Rockwell) under the direction of C. N. Scully [1]. The accelerator used a Li plasma generated by an exploding wire to drag accelerate a cluster of

borosilicate beads with density of 2.2 gm/cm^3. The beads were sized to a precision of ±2.5 percent in diameter using electroformed screens prior to loading. Velocity was measured by observing the time of passage of the bead through an inflight photometer and impact time. Total range length was 4 meters. The photometer also recorded the amplitude of the output of a photomultiplier tube, which viewed the forward scattering of a collimated beam by the particle. This signature can serve as a means of distinguishing undamaged projectiles from fragments and other debris.

The greatest uncertainty in the NAA range is the mass of the impacting projectile, since there is no way of knowing how much material is ablated by the drag acceleration. At first glance, it would appear incredible that a projectile could survive the acceleration process at all. Perhaps the best explanation of the fact that they do survive is that the times involved are extremely short. Since the borosilicate bead is transparent to visible and near ultraviolet, radiation absorption is not significant. Therefore, the only means of transport of energy to the interior is by conduction. Since this is a slow process, only the very outer layers, perhaps only a negligible fraction of the total number of atoms, are affected. There is fairly good evidence, based on comparison of impact craters from this facility with those produced by similar impacts using a different acceleration process, that the beads suffer negligible mass loss.

Unfortunately, the size range that can be accelerated in the NAA facility is too small to perforate the thicker (0.02- and 0.04-cm) Pegasus panels. These tests were performed with a unique explosively driven light gas gun at Hayes International [2,3]. The advantages of this facility are its ability to handle very small projectiles and the low cost per shot. Since many shots are required to establish the ballistic limit (perforation threshold) for a material, and since with these sizes large statistical samples are necessary, this is a factor that cannot be ignored. The Hayes facility uses a very small sabot filled with a cluster of Styrene-divinyl-benzene beads with density of 0.9 gm/cm^3. A small aperture is used as a filter to keep sabot fragments and other debris from contaminating the sample. Velocity is measured by time of flight over a range of approximately 8 meters. Time is taken from gun initiation to impact flash on the front and rear of the sample. For the larger projectiles (>100 microns), inflight photographs were made using Beckman image converter cameras. Velocities attainable in this facility, unfortunately, are limited to around 6 km/sec.

Some attempts were made, using the Hayes facility, to establish the ballistic limit for the very thin samples. In general, these results were in agreement with the NAA results, although there was considerable overlap between perforating and nonperforating conditions, as noted. This is attributed to the difficulty of distinguishing between debris and the extremely small projectiles.

Since the two facilities chosen for the bulk of the testing program used two different projectile materials, a limited number of tests were performed using the conventional light gas gun at ITTRI [4]. This gun was used to sabot launch a single layer of borosilicate beads that had been individually sized under a microscope. The performance was about the same as at the Hayes facility, and the high cost per shot only permitted a few tests for the purpose of confirmation. Velocity of the sabot was measured in a conventional manner, but velocity of the bead was difficult to measure, except in cases of perforation. It was found that the bead velocity, when available, was always somewhat less than the sabot velocity.

After the Hayes tests were completed, an inhouse capability for launching 100-micron glass beads with Space Sciences Laboratory's light gas gun was developed, extending the data for the thicker panels to approximately 8 km/sec.

A summary of all tests is included in the Appendixes.

PREVIOUS BALLISTIC LIMIT WORK

Fish [5], at Ames Research Center, determined ballistic limit data for a variety of materials, including beryllium-copper, 302 stainless steel, 1100-0 aluminum alloy, and 2024-T3 aluminum alloy. The tests were limited to a velocity range from 1.6 to 8.5 km/sec, and a thickness range from 1 to 6 mm, depending on the material. All tests were conducted using 1.59-mm-diameter aluminum spheres. Combining these test results with other results that used different projectile densities and sizes in semi-infinite targets, and assuming the scale in density and size was the same for finite targets as for semi-infinite targets, Fish suggested the perforation formula,

$$T_{(cm)} = 0.65\left(\frac{1}{\epsilon}\right)^{1/18}\left(\frac{\rho_p}{\rho_T}\right)^{1/2} V_{(km/sec)}^{7/8} D_{(cm)}^{19/18}.$$

This can be put in the more convenient form,

$$T_{(cm)} = K\rho_p^{0.418} M^{0.352} V^{0.875} ,$$

where V is in km/sec, M is in gm, ρ is in gm/cm^3, and K is a constant for a given target material, which can be calculated from

$$K \quad \frac{0.816}{\epsilon^{1/18} \rho_T^{1/2}} ,$$

where ϵ is the ductility (percent elongation) and ρ_T is target density. For the targets in question, K has the following values:

Target	ρ	ϵ	K
2024-T3 Al	2.768	0.19	0.538
1100-0 Al	2.71	0.45	0.518
Be-Cu	8.25	0.50	0.295
304 Stainless	8.02	0.50	0.299

EXPERIMENTAL RESULTS

The results of various tests on 0.0025-cm stainless steel samples are shown in Figure 1 with the

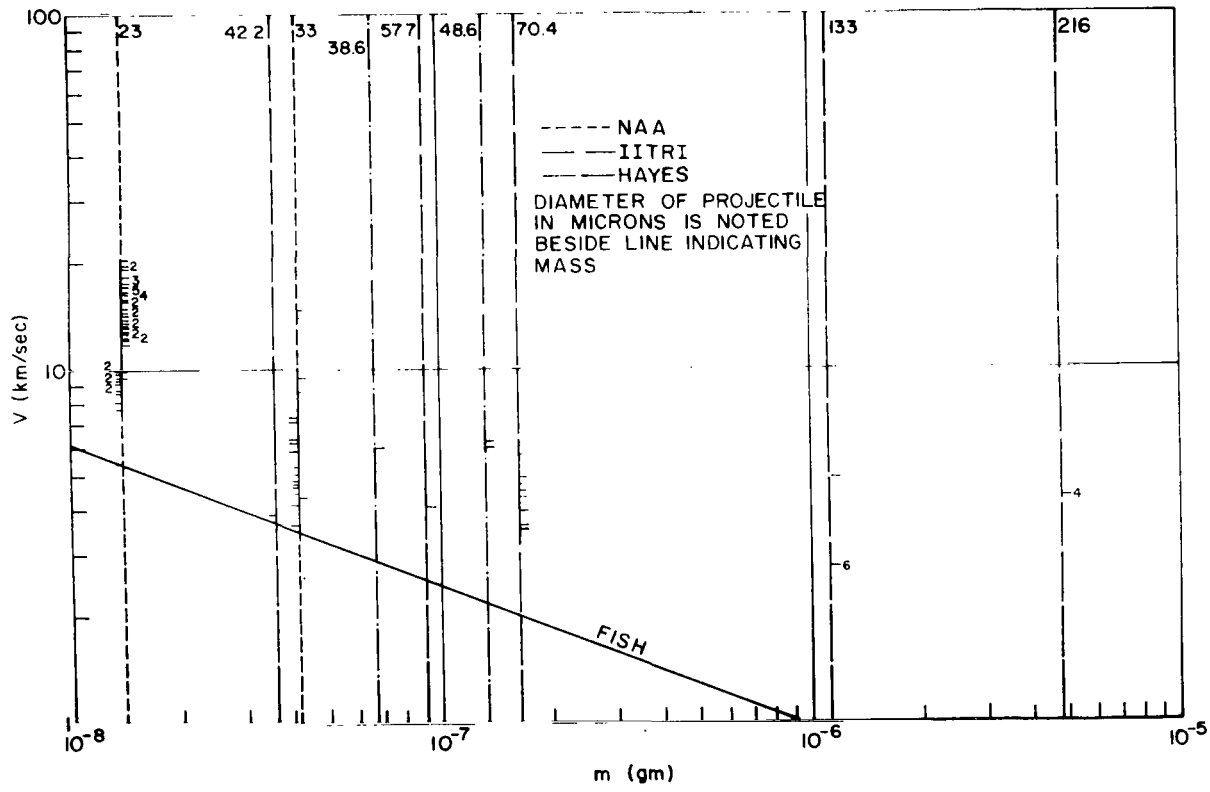

FIGURE 1. RESULTS OF IMPACTS ON A 0.0025-cm STAINLESS STEEL TARGET
(Vertical lines indicate the mass of the projectile. Hash marks indicate the velocity of the projectile and type of impact. Hash marks to the left of the vertical line indicate a nonperforating impact; those to the right a perforating impact.)

predictions calculated from Fish's formula. In presenting these results, a vertical line represents the mass of the series of projectiles. The velocity of a particular projectile is denoted by a short hash mark off the vertical line, to the right if the impact of the particle resulted in perforation, and to the left if it did not. The ballistic limit for the material in question is ideally that line that separates all perforating events from all nonperforating events. In practice, there will be some overlap between perforating and nonperforating conditions arising from variations in sample thickness and microstructure of sample (the fact that some points in the sample are more vulnerable to perforation because of grain structure). The latter effect becomes more pronounced as the thickness approaches grain size. A few cases of severe departure from the bulk of the results, such as the low velocity perforation (5 km/sec) of a 33-micron bead in the 0.0025-cm material when many nonperforations resulted at velocities as high as 7.5 km/sec, are undoubtedly the effect of a large fragment of gun debris.

In presenting the data, it was desirable to be able to compare the NAA data with the Hayes data, even though the two facilities used projectiles of different densities. This was done by assuming the same density dependence as used by Fish, that is,

$$V^{7/8}\,\rho^{0.148} = \text{constant for given mass and thickness} \quad ,$$

and by adjusting the Hayes velocity by a factor

$$V_{adjusted} = V_{actual}\left(\frac{0.9}{2.2}\right)^{0.169}$$

$$V_{adjusted} = 0.86 V_{actual} \quad .$$

Therefore all the figures are adjusted for a projectile density of 2.2 gm/cm^3.

Returning to Figure 1, it is obvious that Fish's formula does not correctly predict the ballistic unit. The large number of shots with 23.8-micron beads by NAA indicate a critical velocity in the vicinity of 11 km/sec. The second series of NAA shots with 33-micron beads tends to place a lower limit of around 8.0 km/sec, while the Hayes and ITTRI tests define upper limits for larger sizes. It is clear that a straight line fit will not accommodate all the data, but there are not sufficient data to justify anything but a straight line fit. Also, since it is necessary to extrapolate the results to high velocities, consideration must be taken of results of other detectors to ensure that the extrapolation is done consistently.

Figure 2 shows the results for the 0.005-cm stainless steel. Again, there seems to be a fairly well-defined point around 13 km/sec for the 33-micron projectiles. Again it may be seen that ballistic limit is above that predicted from the Fish formula, but not as much as was the 0.0025-cm sensor. In both cases, one point is fairly well-defined, but there are not sufficient data to make a good estimate of the slope.

The results of the 0.226-cm and 0.0406-cm Pegasus detector are shown in Figures 3 and 4. Here the consistency is better as the projectiles become more manageable and the fine debris is no longer such a serious problem. It may be seen that the MSFC data are consistent with the Hayes data that has been scaled to account for density. This is indication that the assumed density dependence is not unrealistic. The slope on the ballistic limit consistent with these data appears to be -0.25, indicating a MV^4 dependence. However, the other curves do not seem to indicate velocity dependence this strong. Therefore, for consistency the slope will be taken to be the same as given by Fish's formula. Again, it is evident that the Fish curve is too low, but the difference is considerably less than for the Explorer XXIII stainless steel detectors. This would indicate at first glance that the mass dependence in the Fish formula was incorrect. After all, this mass dependence was borrowed from semi-infinite results, and there is certainly no reason that it must work for ballistic limits as well. Table I lists the threshold velocities for various masses of each example, the thickness T_F predicted from the Fish formula, and the ratio of T_F to actual thickness. It may be observed for the case of 4.13×10^{-8} gm projectiles that the ratio of T_F/T_{actual} is considerably larger for 0.0025-cm targets than for 0.005-cm targets. Therefore, the correction to the Fish formula appears to depend more on thickness of the sensor than on projectile mass. Therefore, it will be assumed that the penetration formula has the form

$$T = f(T)\, T_F$$

where $f(T)$ is a function of thickness only. This retains the mass-velocity-density scaling of the

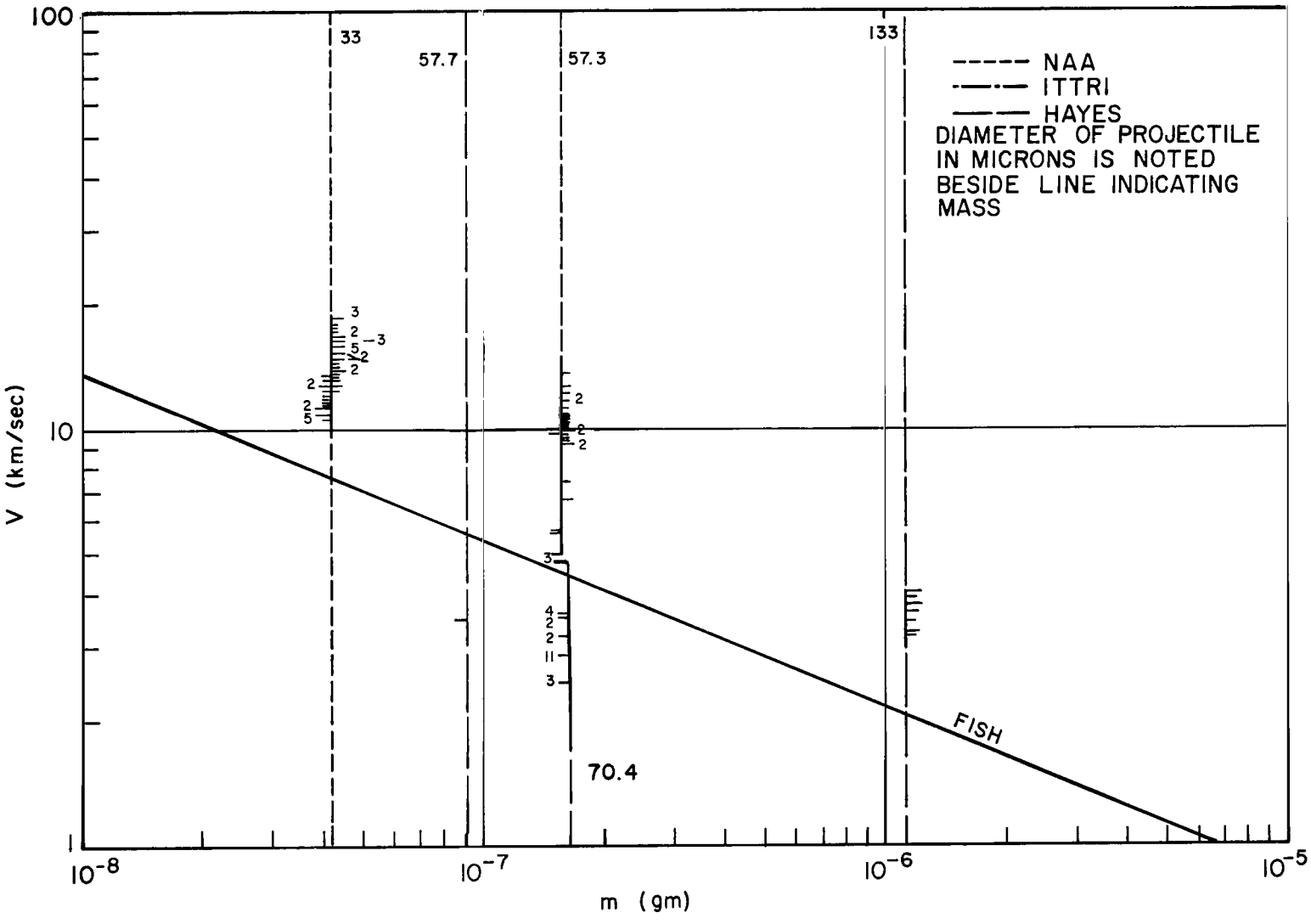

FIGURE 2. RESULTS OF IMPACTS ON A 0.005-cm STAINLESS STEEL TARGET
(Vertical lines indicate the mass of the projectile. Hash marks indicate the projectile's velocity and type of impact. Hash marks to the left of the vertical line indicate a nonperforating impact; those to the right, a perforating impact.)

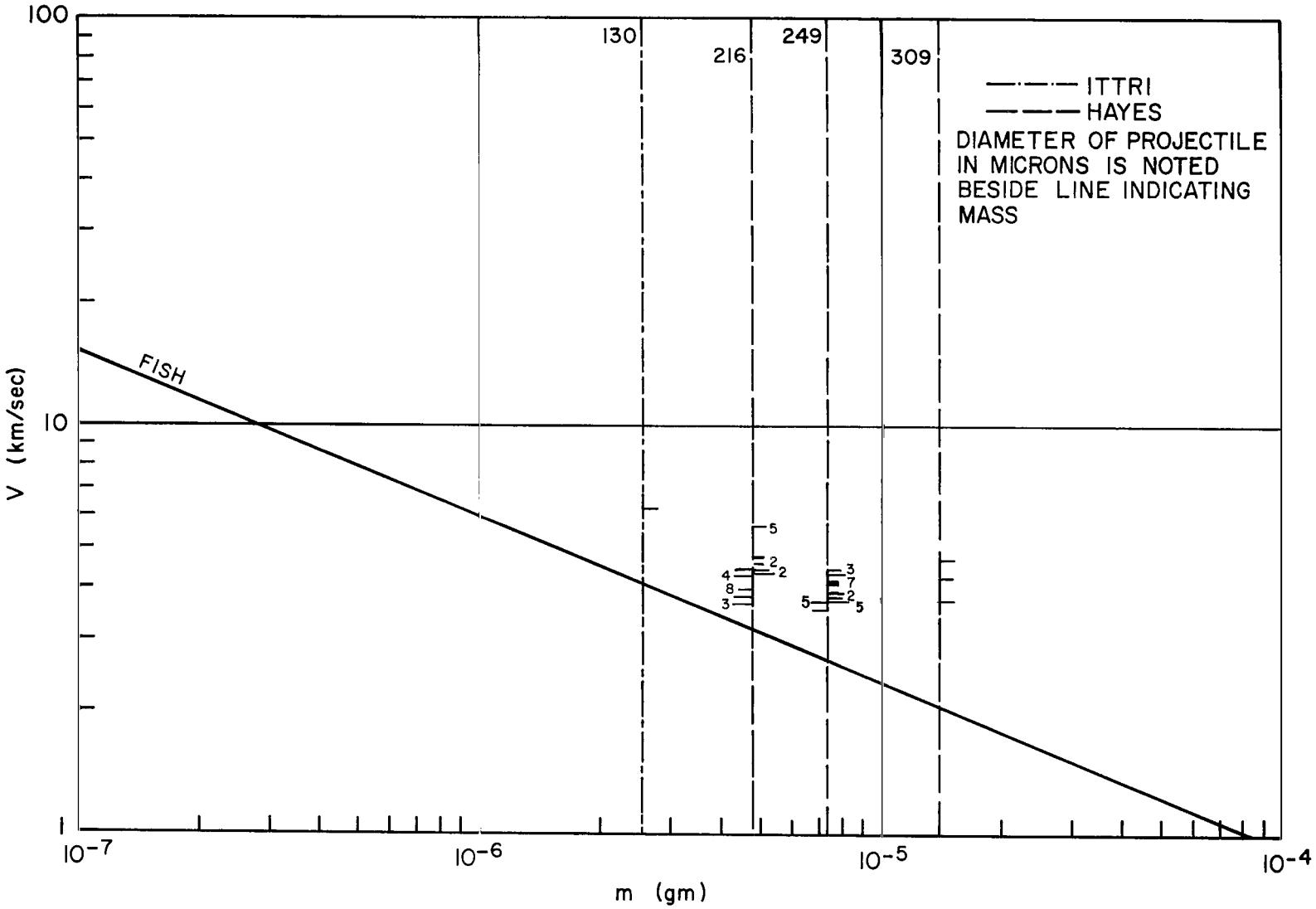

FIGURE 3. RESULTS OF IMPACTS ON A 0.226-cm PEGASUS DETECTOR
(Vertical lines indicate the mass of the projectile. Hash marks indicate the projectile's velocity and the type of impact. Hash marks to the left of the vertical line indicate a nonperforating impact; those to the right, a perforating impact.)

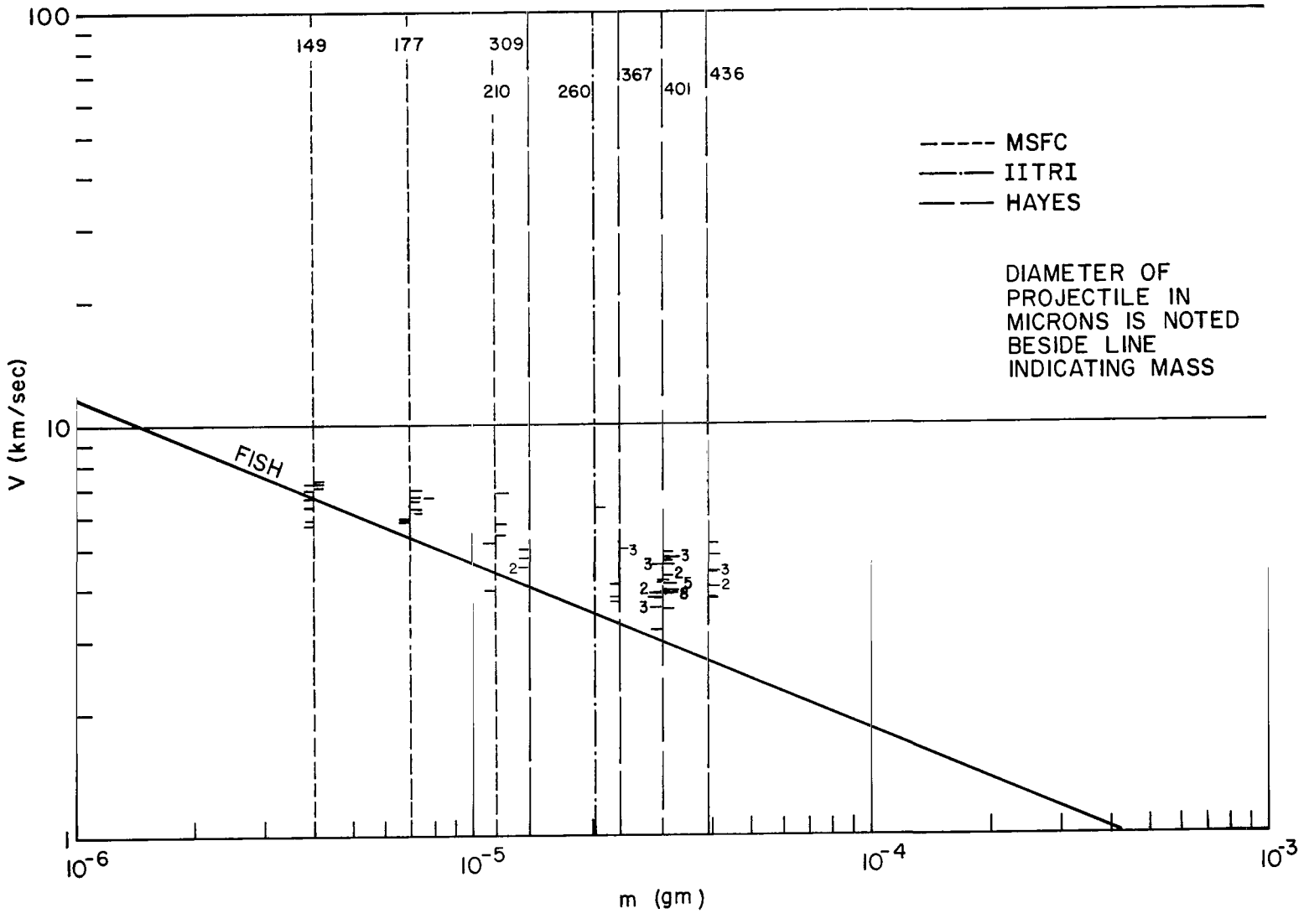

FIGURE 4. RESULTS OF IMPACTS ON A 0.0406-cm PEGASUS DETECTOR

(Vertical lines indicate the mass of the projectile. Hash marks indicate the projectile's velocity and the type of impact. Hash marks to the left of the vertical line indicate a nonperforating impact; those to the right, a perforating impact.)

TABLE I. THRESHOLD VELOCITIES FOR VARIOUS MASSES

Mass	M	ρ	V_T (km/sec)	T_F (cm)	T_F/T		$M_{meteoroid}$ (extrapolated)
0.0025 Stainless	1.4×10^{-8}	2.2	11.0	0.0047	1.89		6.5×10^{-9}
	4.13×10^{-8}	2.2	8.0	0.0052	2.09		8.8×10^{-9}
						Average	7.7×10^{-9}
0.005 Stainless	4.13×10^{-8}	2.2	13	0.008	1.60		2.94×10^{-8}
	1.55×10^{-7}	2.2	< 9.1	<0.0093	<1.87		$<4.55 \times 10^{-8}$
			> 5.6	>0.0061	>1.22		$>1.36 \times 10^{-8}$
						Average	2.95×10^{-8}
0.0226 Aluminum	4.8×10^{-6}	0.9	4.4	0.0263	1.16		2.32×10^{-7}
	7.3×10^{-6}	0.9	3.7	0.0262	1.16		2.30×10^{-7}
						Average	2.31×10^{-7}
0.0406 Aluminum	2.33×10^{-5}	0.9	< 5.0	<0.0515	<1.27		$<1.56 \times 10^{-6}$
			> 4.0	>0.0423	>1.04		$>8.98 \times 10^{-7}$
	3.04×10^{-5}	0.9	3.8	0.044	1.09		1.02×10^{-6}
	3.90×10^{-5}	0.9	< 3.7	<0.047	<1.16		$<1.23 \times 10^{-6}$
	4.2×10^{-6}	2.5	7.24	0.0446	1.10		7.38×10^{-7}
	7.2×10^{-6}	2.5	6.43	0.0486	1.20		9.42×10^{-7}
	1.25×10^{-5}	2.5	5.61	0.0537	1.29		1.16×10^{-6}
						Average	9.6×10^{-7}

Fish formula, that is, the product $M^{0.352}\rho^{0.148}V^{0.875}$ is preserved for a given thickness. Using this and the data in Table I, the meteoroid mass is found from

$$M_{meteoroid} = M_{test}\left(\frac{V_{test}}{V_{meteoroid}}\right)^{2.48}\left(\frac{test}{meteoroid}\right)^{0.42}.$$

The average velocity of meteoroids is taken as 19.17 km/sec, and the average density is taken as 0.5 gm/cm^3. The meteoroid mass characteristic to each detector is

Detector (cm)	Mass (gm)
0.0406 (Pegasus)	9.6×10^{-7}
0.0226 (Pegasus)	2.3×10^{-8}
0.00508 (Explorer XXIII)	2.9×10^{-8}
0.00254 (Explorer XXIII)	7.7×10^{-9}

Two rather surprising results may be noted in the data for the thin stainless steel. Figure 5 is a plot of the penetration depth divided by projectile diameter for 24- and 33-micron projectiles obtained in the North American facility. Notice that there is practically no difference between the two sets of data, indicating almost linear size scaling. However, the ratio of thickness of target to diameter of particle required to perforate that thickness is on the same plot. Notice that this does not even approximately scale linearly with projectile dimensions. At first it was thought that this effect might be caused by excessive mass loss from the 23-micron beads. However, the fact that the craters produced by the same beads do exhibit size scaling negates this possibility. Apparently, this effect is real for these thicknesses, and it is partially responsible for the fact that the observed puncture frequency for the 0.005-cm detector on Explorer XXIII was almost as great as for the 0.00254-cm detector.

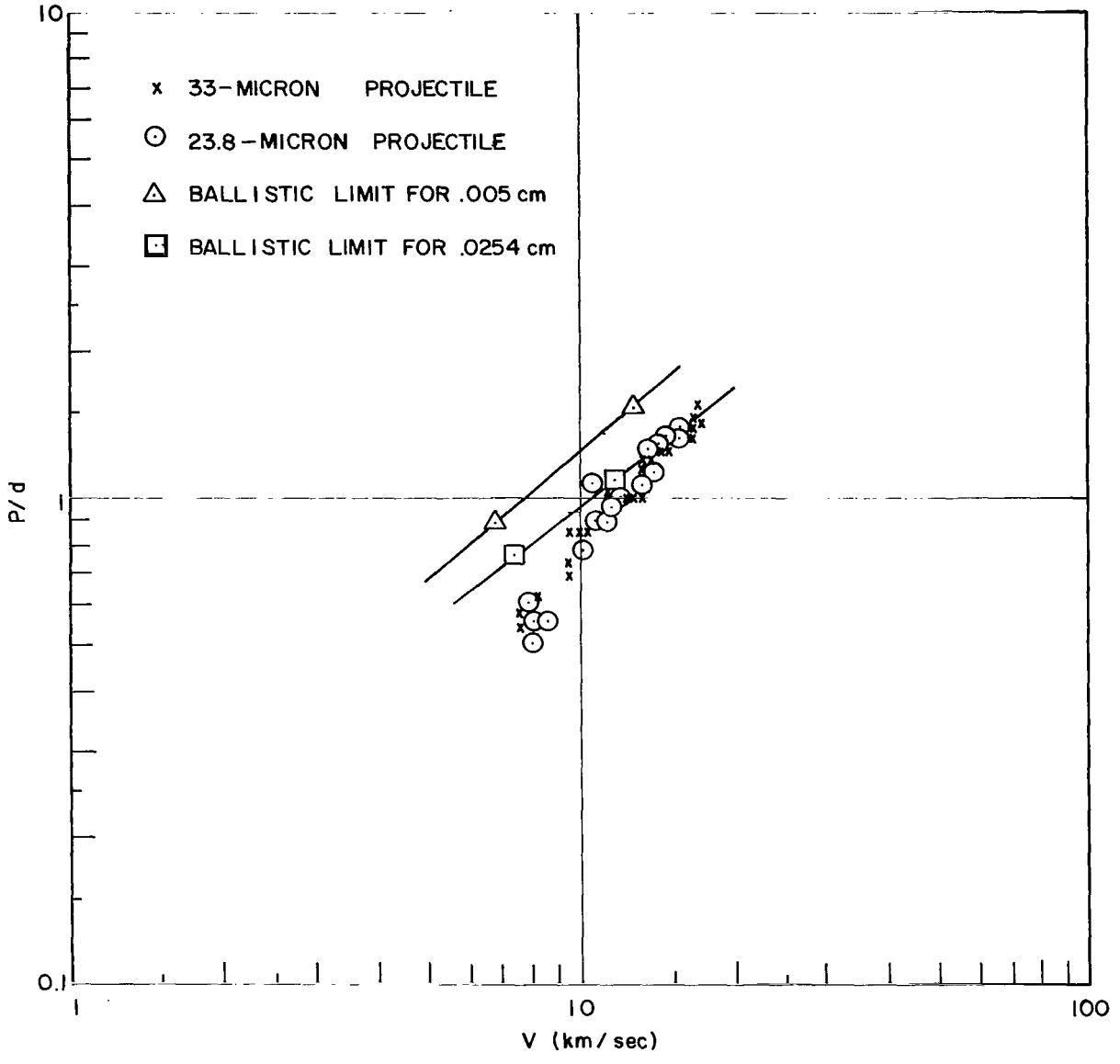

FIGURE 5. COMPARISON OF BALLISTIC LIMIT AND RATIO OF PROJECTILE DIAMETER TO CRATER DEPTH IN SEMI-INFINITE TARGET FOR 304 STAINLESS STEEL

The other surprising feature is that the thickness of material required to stop a projectile appears to approach the crater depth in thick targets as the thickness is reduced. In several instances, craters were observed on the thin sheets with depths exceeding the sheet thickness, indicating that the metal had been drawn in the impact process. Spallation, such as is observed in thicker target materials, was not as evident in the thinner materials. There seems to be little doubt that the mechanisms responsible for perforation of the very thin metals are different from those in the thicker materials for which most of our knowledge of penetration mechanics has been obtained. Therefore, it is not surprising that Fish's penetration equation cannot be extrapolated to thinner materials.

Attempts were made to calibrate the 0.0038-cm 1100-0 aluminum alloy Pegasus detector. This detector is difficult to analyze because it has a thick epoxy backing. This backing materially changes the detector's response to impact, and, in fact, makes it behave more as a semi-infinite solid. The scatter in the data (Fig. 6) makes it difficult to place a ballistic limit. Also, the velocity dependence appears to be considerably different from the thin targets. A crude estimate is indicated by the solid line. Extrapolating this line to 19.17 km/sec and adjusting for density as before, the characteristic mass is estimated to be 3.4×10^{-8} gm.

TESTS OF ELECTRICAL RESPONSE

A large number of preflight tests of Pegasus panels with simulated electronic detection circuitry indicated an overall detection probability of 80 to 90 percent. The majority of these tests were made with a relatively uncontrolled projectile size and were primarily intended as operation assurance tests. The particles impacting the panels ranged from below threshold size to well above threshold size. In fact, the size spectrum was probably not too dissimilar from the actual meteoroid size distribution. Postflight

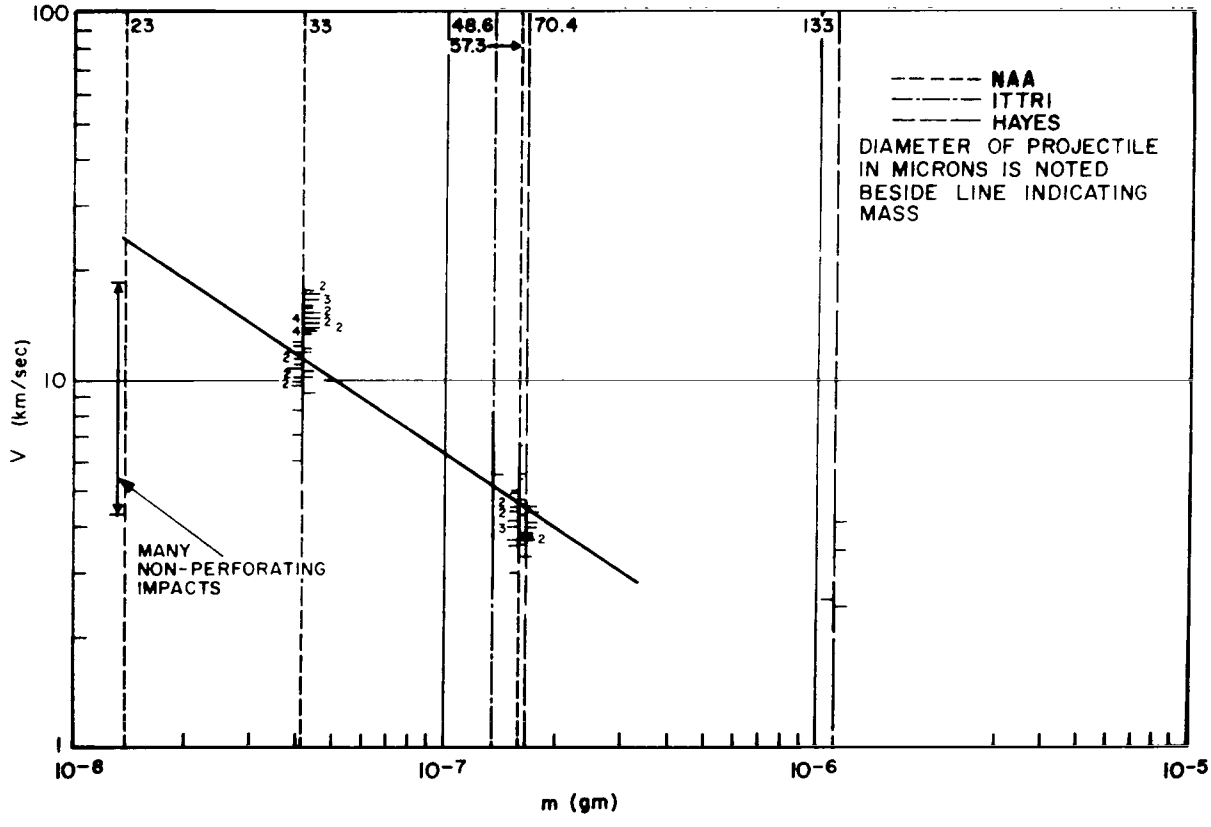

FIGURE 6. RESULTS OF IMPACTS ON A 0.0038-cm PEGASUS DETECTOR
(Vertical lines indicate the mass of the projectile. Hash marks indicate the velocity of the projectile and the type of impact. Hash marks to the left of the vertical line indicate a nonperforating impact; those to the right, a perforating impact.)

tests, in which time was not such a factor, were conducted with controlled particle sizes and flight prototype detection electronics to try to understand what factors affected the detector response. The results of these tests are tabulated in Table II. With several factors such as projectile size, panel temperature, angle of incidence, etc. that apparently affect the operation of the panel, the number of shots required to obtain sufficient statistics to ascertain the detection probability as a function of each of these factors becomes prohibitively large. General trends can be observed from Table II, however. First, it is apparent that detection is marginal for particles near the ballistic limit, particularly if the panel is extremely cold. As the ballistic limit is exceeded, the detection probability rapidly approaches unity. Crude estimates of the functional dependence of detection probability on mass above threshold were integrated over the mass distribution function for meteoroids, with the result that approximately 75 percent of perforating meteoroids will be counted. This is in general agreement with the earlier design assurance tests, which were probably a reasonable simulation of the meteoroid mass distribution. Therefore, the detection probabilities established in the preflight tests will be adopted, since they are based on far better statistics. Since a very limited velocity range (<6.3 km/sec) was available for these tests, it is felt that there is little to be gained in attempting to refine the detection probability until higher laboratory velocities are available.

TABLE II. RESULTS OF DETECTOR TESTS

									Total
Panel Thickness (in.)	0.016	0.008	0.016	0.016	0.016	0.016	0.016	0.016	
Dia. of Bead (μ)	420	420	420	420	595	627	851	851	
Angle of incidence	0	0	0	0	0	30	30	60	
Temperature (°C)	- 40	- 40	50	25	25	25	25	25	
Single perforations	2	3	3	8	6	4	6	6	38
Number detected	0	3	3	4	6	3	5	3	27
% detected	0	100	100	50	100	75	83	50	71
Shorts	0	0	0	0	1	1	0	1	3
% shorts	0	0	0	0	16.7	25	0	17	8
Multiple perforations	6	3	4	10	2	3	1	0	29
Number detected	5	3	3	9	2	3	1	0	26
% detected	83	100	75	90	100	100	100	0	90
Shorts	1	0	0	5	0	0	1	0	7
% shorts	17	0	0	50	0	0	100	0	24
Nonperforations	8	0	4	11	0	0	0	3	26
Number detected	0	0	2[a]	2[a]	0	0	0	0	4
% detected	0	0	50	18	0	0	0	0	14
Shorts	0	0	0	0	0	0	0	0	0
% shorts	0	0	0	0	0	0	0	0	0

a. Near threshold events.

George C. Marshall Space Flight Center
National Aeronautics and Space Administration
Marshall Space Flight Center, Alabama 35812,

July 14, 1969 124-09-15-00-62

APPENDIX A

SUMMARY OF THE FIRST SERIES OF CALIBRATION TESTS AT NORTH AMERICAN ROCKWELL[1]

INTRODUCTION

The experimental program described in this report had two objectives. The first was the determination, by a series of hypervelocity impacts, of the threshold velocity for perforation of specific materials impacted by artificial micrometeoroids. The threshold velocity for perforation is customarily referred to as the ballistic limit or the minimum velocity at which a specific projectile is capable of producing a perforation in a particular thin target. The materials of interest in this program were those employed in previous micrometeoroid measurement satellite experiments. The second objective was the determination of the projectile diameter to impact crater depth ratio for craters produced in semi-infinite targets of the same material composition and physical properties as the thin sheet targets studied in the first objective, over a range of velocities encompassing the threshold perforation velocity for the thin sheet experiments.

TARGET MATERIALS

The target materials were supplied by the George C. Marshall Space Flight Center and consisted of Type 302 corrosion resistant steel in the half-hard condition in thickness of 0.001- and 0.002-in. and a nominal 0.0015-in. capacitor from the perforation sensor layer of a Pegasus micrometeoroid perforation detection satellite panel. In addition, 2- by 2- by 0.375-in. 302 CRES, reportedly in the same heat treat condition as the thin sheet material, and 1.5- by 1.5- by 0.105-in. 1100-0 aluminum were employed.

EXPERIMENTAL TECHNIQUES

The firing experiments were conducted in North American Aviation's Mark IV Electrothermal Gun System in its Space Sciences Department, Space and Information Systems Division, Downey, California. The gun system, which accelerates spherical silicate projectiles with a diameter range of 20 to 90 microns by aerodynamic drag forces produced by a dense flowing plasma, has been described in a series of previous reports. The most complete description appears in the Proceedings of the Seventh Hypervelocity Impact Symposium.

The method for determining the threshold perforation velocity was to provide a series of impacts over a wide range of velocities in a number sufficient to clearly define the minimum velocity projectile capable of producing a perforation. To determine the threshold velocity, the targets were mounted within the hypervelocity range target chamber with two viewing photomultiplier tubes. The field of view of the first photomultiplier tube was restricted to the front surface of the target material and detected the luminous impact flash. The impact flash signal was recorded on one channel of a two-beam oscilloscope, Tektronix 551 with Type K pre-amplifier. The field of view of the second photomultiplier was restricted to the rear surface of the target, and, in the event that a perforation took place, a luminous flash from the rear surface was detected and recorded on the second channel of the two-beam oscilloscope. Coincidences of impact flash and rear surface flash were evidence that the incident projectile had produced a perforation. All other range instrumentation techniques have been described in the referenced source.

It was a restriction in the statement of work that the projectile diameters be such that the threshold perforation velocity was in excess of 10 km/sec (32 800 fps). For this reason each of the thin sheet target materials was subjected to impacts by borosilicate glass spherical projectiles (density 2.23) over a range of velocities to determine which projectile diameters would be used for the acquisition of impact data for the perforation experiments. The projectile diameters chosen for the principal experiments were 22.9 microns (0.0009 in.), 33.0 microns

1. Calculations in Appendixes A through D were not made according to the International System of Units, since the contractors for these tests were not bound by NASA regulations. Raw data were received directly from the test centers and follow in Appendixes through D.

(0.0013 in.), and 51.4 microns (0.00202 in.). Standard deviation from the mean diameter was 2.5 percent.

The thin sheet 302 CRES was used in the "as received" condition. Precision measurements of received material indicated an actual thickness of 0.0018 in. for the nominal 0.002 in. CRES and 0.0009 in. for the nominal 0.001 in. The Pegasus sensor material was received in the form of a flight-type 20- by 40-in. double surface panel. The full-scale panel was cut into 2-in. squares, and the plastic foam backing was removed from the capacitor. The adhesive bonding material used to join the capacitor to the plastic foam panel remained on the capacitor surface. The target sheet therefore consisted of a multi-layered structure of 0.0015-in. aluminum, a bonded Mylar layer, a vapor-deposited copper layer, and a layer of adhesive. The overall average thickness was 0.0019 in. This fact is significant in the interpretation of the perforation threshold data.

PERFORATION THRESHOLDS

Based upon the determination of the projectile diameters, whose impacts lead to perforations at velocities above 32 800 fps, a series of firings was conducted for each of three specific thin sheet targets.

The results of the perforation experiments for 0.0013-in.-diameter spheres on 0.0015-in. Pegasus detector panels is summarized in Table A-I. A total of 30 perforations was obtained over a range of velocities from 57 300 fps down to 39 400 fps. No perforations were obtained at any velocities below 39 400 fps, and this value may be considered as the threshold velocity for perforations for this specific combination of projectile and target materials. The summary of perforation experiments for 0.0009-in. diameter projectiles on 0.001-in. 302 CRES is summarized in Table A-I. A total of 35 perforations was obtained over the velocity range from 65 000 fps down to 38 800 fps. No perforations were obtained with any impacts below the lower limit. Table A-I summarizes the perforation experiments with 0.0013-in. diameter projectiles on a 0.002-in. 302 CRES, where a total of 30 perforations were obtained over the velocity range from 60 200 fps down to 40 100 fps.

SEMI-INFINITE TARGET IMPACTS

It is the objective of this particular task to determine the ratio of crater depth to projectile diameter for each of the target materials and for each of the combinations of projectile diameters and target materials at the penetration threshold velocity for the thin sheet targets. To accomplish this end, a series of firings were conducted with appropriately sized projectiles on each of the target materials and the crater depth to projectile diameter ratio determined for each impact for which there was range indication that the impact was produced by an intact projectile. Table A-II summarizes the values of p/d for each of 31 craters obtained over an impact velocity range of 49 800 fps down to 15 400 fps for 0.0013-in. diameter projectiles on 1100 aluminum. Table A-III summarizes similar measurements for the 32 impact craters produced by 0.0009-in. diameter projectiles on 302 CRES over the velocity range from 54 300 fps to 24 900 fps. Similarly, Table A-IV gives equivalent data for the 31 craters produced by 0.0013-in. diameter spheres on 302 CRES of 56 800 fps down to 24 900 fps.

MISCELLANEOUS FIRINGS

During the first portion of the effort, which consisted of a series of impact experiments on thin sheet targets for determining the appropriate diameter of projectiles to be employed for the main body of firings, certain data points were obtained using different combinations of projectile diameters and targets than those employed in the main program. While the results of these firings indicated that the projectile diameter was such that the penetration threshold was below the desired value of 32 800 fps, the data is considered to have some value for the interpretation of both the laboratory experiments and the behavior of certain materials under space meteoroid impact. The results of these firings are summarized in Table A-V.

SUMMARY

The p/d values for those impacts obtained at the penetration threshold velocity for each combination of projectile and target materials may be determined by drawing a smooth curve through the individual p/d values over the full velocity ranges indicated in Tables A-II, A-III, and A-IV. An anomalous result is noticed in the case of the 0.0015-in. Pegasus capacitor target. At the threshold perforation velocity of 39 400 fps, the corresponding p/d in the semi-infinite material is 2.04. If one assumes that the target material is basically 0.0015-in. aluminum, this would lead to a ratio of the thickness of the thin target material to the depth of penetration in the semi-infinite material of 0.56. This result cannot be accepted as having any significance. It should be remembered that the capacitor target was a composite target of four different materials, three of which have appreciable thickness. The influence of the adhesive bonding material used to provide adherence of the capacitor structure to the 1-in. thick plastic foam is not negligible and appears to significantly increase the resistance to perforation by projectiles of the diameter used in the experiments.

TABLE A-I. IMPACT VELOCITIES LEADING TO PERFORATION

Velocity,[a] fps	Firing Reference No.[a]	Velocity,[b] fps	Firing Reference No.[b]	Velocity,[c] fps	Firing Reference No.[c]
57 300	8194	65 000	8012	60 200	8069
56 100	7953	63 300	8017	60 200	8070
56 100	8207	63 300	8035	60 200	8074
54 700	7944	60 200	8007	58 700	8077
54 700	7953	57 300	8033	57 300	8081
54 700	7957	56 100	8018	56 100	8055
52 300	7976	56 100	8020	54 700	8120
52 200	7944	56 100	8041	54 700	8120
50 100	7948	54 700	7983	53 500	8071
50 100	7952	54 700	8001	53 500	8083
49 100	7948	54 700	8009	53 500	8120
49 100	7952	53 700	8013	52 300	8062
49 100	8217	52 700	8023	52 300	8063
49 100	8225	52 300	8003	52 300	8096
48 100	7952	52 300	8013	52 300	8121
48 100	7953	52 300	8029	52 300	8121
48 100	8324	52 300	8043	50 100	8060
48 100	8325	51 200	8003	50 100	8096
47 200	7949	51 200	8035	49 100	8066
47 200	7969	49 100	8014	49 100	8085
46 300	7947	48 100	8010	48 100	8124
46 300	8324	48 100	8031	47 200	8097
45 400	7972	46 300	8013	46 300	8108
45 400	8221	45 400	8037	45 400	8121
45 400	8224	43 000	7978	43 700	8101
43 400	8324	42 200	8024	43 000	8061
44 600	7943	41 500	8013	42 200	8097
43 000	8217	41 500	7983	41 500	8060
40 100	8320	40 800	7978	40 100	8112
39 400	8224	54 700	8315		
		46 300	8314		
		44 600	8313		
		43 700	8313		
		43 700	8314		
		38 800	8317		

a. Panel: 0.0015-in. Pegasus detector
Projectile: 0.0013-in-diameter borosilicate spheres

b. Panel: 0.001-in. half-hard 302 CRES
Projectile: 0.0009-in.-diameter borosilicate spheres

c. Panel: 0.002-in. half-hard 302 CRES
Projectile: 0.0013-in.-diameter borosilicate spheres

TABLE A-II. PENETRATION DEPTH TO PROJECTILE DIAMETER RATIO[a]

Crater Depth to Projectile Dia. Ratio	Impact Velocity fps	Firing Reference No.
2.23	49 800	8338
1.92	37 000	8343
1.69	30 900	8343
1.39	22 800	8344
1.69	32 100	8348
1.69	31 700	8348
1.85	34 900	8348
1.66	30 100	8348
2.08	38 800	8348
1.77	33 400	8348
1.62	29 800	8348
1.15	15 400	8348
1.31	20 700	8348
1.62	28 100	8348
1.92	36 400	8348
2.08	39 400	8348
1.92	37 000	8348
1.58	27 700	8348
1.62	27 700	8350
2.23	45 200	8350
1.81	33 900	8350
2.00	39 400	8350
2.08	42 200	8354
1.85	35 400	8354
1.31	22 200	8354
1.46	24 900	8358
1.38	24 700	8358
1.54	27 800	8363
1.00	15 900	8351
1.15	20 000	8351
1.15	18 900	8351

a. Panel: 1100 aluminum
Projectile: 0.0013-in.-diameter borosilicate spheres

TABLE A-III. PENETRATION DEPTH TO PROJECTILE DIAMETER RATIO[a]

Crater Depth to Projectile Dia. Ratio	Impact Velocity fps	Firing Reference No.
1.33	54 300	8421
1.28	47 000	8422
1.28	50 800	8426
1.22	48 700	8426
0.555	28 100	8426
0.555	26 800	8426
0.50	26 500	8426
0.555	28 100	8427
1.00	40 000	8428
0.445	24 900	8430
0.78	33 000	8430
0.61	29 800	8430
0.61	26 200	8430
1.11	43 700	8430
0.555	25 400	8430
0.61	26 000	8430
1.00	39 400	8430
1.33	52 000	8431
1.33	49 700	8436
0.89	35 900	8437
1.22	44 400	8442
1.39	52 100	8445
1.00	41 500	8445
0.945	38 200	8446
0.89	37 600	8446
1.00	39 400	8446
1.22	45 300	8446
1.06	43 700	8446
1.11	45 300	8450
1.11	43 700	8451
1.34	48 700	8451
1.22	46 000	8458

a. Panel: 302 CRES
Projectile: 0.0009-in.-diameter borosilicate spheres

TABLE A-IV. PENETRATION DEPTH TO PROJECTILE DIAMETER RATIO[a]

Crater Depth to Projectile Dia. Ratio	Impact Velocity fps	Firing Reference No.
1.38	56 800	8379
1.31	49 700	8383
1.23	45 300	8383
1.16	45 300	8389
1.11	43 500	8389
1.16	44 400	8389
1.00	41 500	8389
1.23	47 000	8389
1.16	46 000	8389
1.23	46 000	8389
1.00	40 700	8391
0.85	33 400	8391
0.695	31 000	8391
0.85	32 600	8391
0.73	31 300	8391
0.54	24 400	8391
0.615	26 600	8391
0.575	25 200	8391
0.615	26 600	8394
0.54	24 900	8394
1.23	47 000	8394
0.54	24 700	8394
0.85	31 700	8396
1.08	42 700	8396
1.23	48 700	8396
1.00	38 200	8396
1.23	46 000	8396
1.31	54 300	8398
1.54	55 500	8407
1.39	54 300	8407
1.46	55 500	8413

a. Panel: 302 CRES
Projectile: 0.0013-in.-diameter borosilicate spheres

TABLE A-V. PRELIMINARY IMPACT VELOCITY TESTS

Panel Thickness (in.)	Projectile Dia. (in.)	Velocity (fps)	Firing Reference No.
0.0015[a]	0.0009[b]	c	c
0.001[d]	0.0013[b]	49 100	7996
		46 200	7996
		28 300	7997
		14 200	7997
0.002[d]	0.00202[b]	45 400	8049
		41 500	8049
		40 100	8048
		40 100	8051
		39 400	8053
		37 600	8045
		36 500	8053
		36 000	8051
		35 400	8047
		34 900	8047
		30 900	8052

a. Pegasus detector panel

b. borosilicate spheres

c. No perforations were obtained with any impacts between 14 000 and 60 000 fps

d. half-hard 302 CRES

APPENDIX B

SUMMARY OF THE SECOND SERIES OF CALIBRATION TESTS AT NORTH AMERICAN ROCKWELL

INTRODUCTION

The comparison of satellite data providing estimates of the meteoroid penetration flux in the near-earth environment obtained from different types of meteoroid perforation detectors is complicated by two facts. One, perforation detectors, such as the capacitor discharge type employed in the Pegasus satellites and the pressurized container type employed in the Explorer series of satellites, are operated by different mechanisms in signalling perforating events and the sensors are composed of materials whose composition, thickness, and structure are not identical. The second fact is that the perforation threshold for different masses and velocities of micrometeoroids for the several types of sensor materials has not been well established. Laboratory experiments have been and are being conducted to subject the several sensor target materials to perforating and nonperforating impacts with artificial micrometeoroids under identical conditions. That velocity at which a given micrometeoroid mass provides a 50 percent probability of producing a perforation in a given thin target is the ballistic limit.

Under a previous contract, NAS8-21007, with a title identical to the current contract, "Experimental Hypervelocity Impact Research," a series of hypervelocity impact firings were conducted in the contractor's Mark IV Electrothermal Gun System to determine the ballistic limit for a series of thin single sheet targets when impacted by borosilicate glass spheres of specified diameters. The previous program was more exploratory in nature, since the ballistic limit, or the minimum velocity at which a specific projectile is capable of producing a perforation in the particular thin targets, was not known within rather broad limits. After the previous program had established ballistic limits, the George C. Marshall Space Flight Center desired a more precise determination of the ballistic limit of some of the older, and one new material. This goal under the current contract was reached by conducting a large number of firings with projectiles having a velocity range within narrow limits so that the boundary line between the perforation, nonperforation condition could be established with a lesser degree of uncertainty. Only a small proportion of firings conducted would fall within the narrower limits.

TARGET MATERIALS

The target materials were supplied by the George C. Marshall Space Flight Center and were, with one exception, identical to those employed in a previous contract. These consisted of thin sheets of Type 302 corrosion resistant steel in the half-hard condition in 0.001-in and 0.002-in. thickness, and the nominal 0.0015-in. capacitor from the perforation sensor layer of a Pegasus micrometeoroid perforation detection satellite panel. In addition, a 0.002-in. thickness beryllium-copper sheet was supplied as an additional target material.

EXPERIMENTAL TECHNIQUES

The firing experiments were in all respects identical to those conducted and reported in the Final Technical Report on contract NAS8-21007. The projectile diameters of the borosilicate glass spheres were to be normally 20, 30, and 50 microns. The actual diameters, based upon microscopic measurement, were 22.9 microns (0.00090 in.), 33.0 microns (0.0013 in.), and 51.4 microns (0.00202 in.).

The diameters, determined from measurements of 20 randomly selected spheres, are mean values with a standard deviation of the mean of 2.5 percent.

All projectiles are monitored in flight to determine that the impacts reported were produced by intact spherical projectiles. Evidence for a perforating impact was provided by the simultaneous recording of a front surface and rear surface impact flash as well as a postfiring microscopic examination of the target.

The velocity ranges of interest for each projectile-target combination were

25 to 42 000 fps for 20-micron spheres on 0.001-in. CRES

12 to 25 000 fps for 30-micron spheres on 0.001-in. CRES

35 to 45 000 fps for 30-micron spheres on 0.002-in. CRES

18 to 36 000 fps for 50-micron spheres on 0.002-in. CRES

35 to 45 000 fps for 30-micron spheres on 0.002-in. Be-Cu

18 to 36 000 fps for 50-micron spheres on 0.002-in. Be-Cu

20 to 42 000 fps for 30-micron spheres on 0.0015-in. Pegasus

12 to 20 000 fps for 50-micron spheres on 0.0015-in. Pegasus .

For each target-projectile combination, 18 impacts were obtained with intact projectiles of known dimensions within each specified velocity range. In addition, two impacts, one above and one below the indicated velocity range, were obtained for each projectile-target combination.

The firing results are reported in Table B-I, preceded by an explanation of the data.

SUMMARY

The results of the program are contained in the table of data giving the firing results and observations for the eight projectile-target combinations. Several particular points are of interest. In a large number of cases where a nonperforating impact occurred, the measured depth of the crater exceeds the original thickness of the target sheet. This type of event occurs more regularly in ductile materials. Bulging of the rear surface of the target sheet frequently accompanies nonperforating penetrations.

Attention is directed to the fact that the 0.0015-in. Pegasus capacitor material is a complex multilayered structure whose total thickness is greater than the nominal 0.0015-in. aluminum sheet. In addition to the aluminum, there is the Mylar dielectric with a vapor-deposited copper layer. Since the capacitor material was removed from the plastic foam backing, there remained the foam bonding adhesive layer whose thickness is not constant over a large area. The ballistics data report under this program cannot be used for estimating the threshold velocity for perforation of pure aluminum targets.

For some projectile-target combinations the threshold velocity lay outside the designated velocity range.

Visual observations of unusual appearance of impact sites are included in the tables. Several cases were observed where the bottom of the crater had a perforation in the form of an irregular tear rather than a round hole.

HYPERVELOCITY IMPACT FIRINGS

Explanation of Table B-I

Column 1 firing reference number

Column 2 number of projectiles passing projectile monitor station

Column 3 number of impact craters on target

Column 4 number of perforations in target due to intact projectiles

Column 5 depth of crater produced by intact projectile (in.)

Column 6 diameter of crater or perforation (in.)

Column 7 projectile integrity as determined from projectile monitor signal

Column 8 time of flight from launch to projectile monitor station (microseconds)

Column 9 time of flight of projectile from launch to impact on target at 12.50 foot station

Column 10 computed projectile velocity over 12.5 foot distance (fps)

Column 11 visual observation of perforation

Column 12 comments

TABLE B-I. HYPERVELOCITY IMPACT FIRING RESULTS

Target material: 0.001-in. single sheet 302 CRES (half-hard)
Projectile: 0.0009-in.-diameter borosilicate spheres

1	2	3	4	5	6	7	8	9	10	11	12
8626-1	4	4	0	0.00065	0.0012	Intact	225	370	32 500		
8626-2				0.0004	0.001	Intact	260	430	28 000		
8728-1	3	3	0	0.00055	0.0016	Intact	215	350	34 400		
8728-2				0.0005	0.0014	Intact	235	380	31 600		
8732-1	4	2	0	0.0005	0.0013	Intact	290	480	25 000		
8732-2				0.0003	0.0009	Intact	415	680	17 700		This point below velocity limit.
8761-1	1	1	0	0.0009	0.0017	Intact	235	380	31 600		
8751-1	1	1	0	0.00045	0.0013	Intact	250	405	29 700		
8713-1	4	4	0	0.0006	0.00125	Intact	278	450	26 700		
8711-1	7	5	0	0.00055	0.0013	Intact	240	395	30 500		
8711-2				0.00045	0.0012	Intact	255	420	28 600		
8711-3				0.0004	0.0011	Intact	280	455	26 400		
8733-1	13	13	1	0.00095	0.0016	Intact	212	345	34 900		
8733-2				Perf.	0.0018	Intact	228	370	32 500	Regular	
8733-3				0.00075	0.0015	Intact	238	385	31 300		
8733-4				0.00055	0.0012	Intact	245	400	30 100		
8719-1	1	1	0	0.0005	0.00125	Intact	242	395	30 500		
8718-1	13	13	1	0.0013	0.0015	Intact	225	370	32 500		
8718-2				Perf.	0.00135	Intact	240	390	30 900	Barely perforated	
8822-1	4	4	1	Perf.	0.0015	Intact	175	280	43 000	Regular	This point above velocity limit.

TABLE B-I. (Continued)

Target material: 0.001-in. single sheet 302 CRES (half-hard)
Projectile: 0.0013-in.-diameter borosilicate spheres

1	2	3	4	5	6	7	8	9	10	11	12
8628-1	10	9	0	0.00045	0.0012	Intact	350	575	20 900		
8628-2				0.0004	0.0011	Intact	455	740	15 600		
8630-1	12	12	1	Perf.	0.0016	Intact	240	390	30 900	Regular	This point above velocity limit.
8630-2				0.0007	0.0014	Intact	308	500	24 100		
8630-3				0.00035	0.0012	Intact	378	615	22 100		
8632-1	7	7	0	0.0006	0.00145	Intact	330	535	22 500		
8632-2				0.00055	0.0014	Intact	363	590	20 400		
8632-3				0.00035	0.0012	Intact	445	725	16 600		
8632-4				0.00035	0.00105	Intact	485	790	15 200		
8638-1	8	6	0	0.0004	0.0014	Intact	318	515	23 400		
8638-2				0.00035	0.0011	Intact	460	745	16 100		
8638-3				0.0003	0.0010	Intact	510	825	14 600		
8643-1	5	5	0	0.00055	0.0018	Intact	385	625	19 200		
8643-2				0.0005	0.0012	Intact	460	750	16 000		
8643-3				0.0003	0.0010	Intact	615	1010	11 900		This point below velocity limit.
8648-1	5	5	0	0.0005	0.0014	Intact	340	550	21 900		
8647-1	4	4	0	0.0003	0.0011	Intact	485	790	15 200		
8659-1	5	4	0	0.00045	0.0015	Intact	400	650	18 500		
8663-1	3	3	1	0.00035	0.0012	Intact	542	880	13 700		One perforation on target was above velocity limit. Data not recorded.
8665-1	6	6	0	0.00045	0.0012	Intact	435	705	17 100		

TABLE B-I. (Continued)

Target material: 0.002-in. single sheet 302 CRES (half-hard)
Projectile: 0.0013-in.-diameter borosilicate spheres

1	2	3	4	5	6	7	8	9	10	11	12
8670-1	1	1	0	0.0008	0.0012	Intact	330	530	22 700		This point below velocity limit.
8780-1	18	18	0	0.0018	0.0032	Intact	165	270	44 600		
8783-1	7	7	0	0.0016	0.0026	Intact	180	280	43 000		
8784-1	10	10	0	0.0012	0.0021	Intact	210	340	35 400		
8788-1	6	6	0	0.0015	0.0022	Intact	198	315	38 200		
8823-1[a]	4	3	0	0.0023	0.0025	Intact	180	290	41 500		
8827-1	18	18	0	0.0013	0.0021	Intact	210	340	35 400		
8828-1	2	2	0	0.0013	0.0021	Intact	200	325	37 000		
8832-1	20	20	1	Perf.	0.00265	Intact	160	260	46 300	Regular	This point above velocity limit.
8839-1	10	10	0	0.0015	0.0025	Intact	180	290	41 500		
8840-1	7	7	0	0.0011	0.0020	Intact	190	340	35 400		
8843-1	9	9	0	0.00125	0.0022	Intact	190	310	38 800		
8843-2				0.0012	0.0021	Intact	210	340	35 400		
8859-1	3	3	0	0.00125	0.0022	Intact	180	305	37 400		
8870-1	9	9	0	0.00125	0.0025	Intact	200	340	35 400		
8878-1	7	6	0	0.0014	0.0027	Intact	188	305	39 400		
8890-1	11	11	1	0.0018	0.0029	Intact	180	290	41 500	Regular	
8890-2				Perf.	0.0027	Intact	183	300	40 100		
8890-3				0.00135	0.0021	Intact	200	325	37 000		
8903-1	11	11	0	0.00115	0.002	Intact	215	345	35 000		

a. Prior to firing 8823, lamp in projectile monitor was changed and monitor recalibrated.

TABLE B-I. (Continued)

Target material: 0.002-in. single sheet 302 CRES (half-hard)
Projectile: 0.00202-in.-diameter borosilicate spheres

1	2	3	4	5	6	7	8	9	10	11	12
8926-1	16	16	3	Perf.	0.0044	Intact	225	370	32 500	Regular	
8926-2				Perf.	0.0040	Intact	250	400	30 100	Regular	
8926-3				Perf.	0.0038	Intact	270	450	26 700	Regular	
8946-1	8	5	1	Perf.	0.0040	Intact	245	400	30 100	Regular	
8952-1	8	8	4	Perf.	0.0039	Intact	215	350	34 400	Regular	
8952-2				Perf.	0.0038	Intact	220	360	33 400	Barely perforated	
8952-3				Perf.	0.0036	Intact	235	380	31 600	Barely perforated	
8955-1	12	6	1	Perf.	0.0048	Intact	190	305	39 400	Regular	This point above velocity limit.
8971-1	13	13	1	Perf.	0.004	Intact	335	540	22 300	Barely perforated	
8971-2				0.0014	0.003	Intact	460	745	16 100		This point below velocity limit.
8974-1	8	8	0	0.0015	0.0032	Intact	405	655	18 400		
8989-1	18	18	0	0.0026	0.0034	Intact	230	375	32 100		
8989-2				0.0014	0.0032	Intact	395	645	18 700		
8990-1	7	7	3	Perf.	0.0041	Intact	245	400	30 500	Regular	
8990-2				Perf.	0.0040	Intact	290	480	25 000	Regular	
8990-3				Perf.	0.0035	Intact	295	485	24 800	Barely perforated	
8995-1	15	15	4	Perf.	0.0042	Intact	215	355	33 900	Regular	
8995-2				Perf.	0.0041	Intact	225	365	33 000	Regular	
8995-3				Perf.	0.0040	Intact	230	370	32 500	Regular	
8995-4				0.002	0.0038	Intact	270	440	27 300	Regular	

TABLE B-I. (Continued)

Target material: 0.002-in. single sheet beryllium-copper (half-hard)
Projectile: 0.00013-in.-diameter borosilicate spheres

1	2	3	4	5	6	7	8	9	10	11	12
9000-1	4	4	2	Perf.	0.0047	Intact	180	290	41 500	Regular	Above velocity limit.
9001-1	19	19	2	Perf.	0.0043	Intact	195	315	38 000	Regular	
9001-2				0.0025	0.0036	Intact	240	390	30 900		
9001-3				Perf.	0.0042	Intact	245	405	29 700	Regular	
9001-4				0.00225	0.0036	Intact	295	480	25 000		
9002-1	13	10	4	Perf.	0.0045	Intact	198	360	33 400	Regular	
9002-2				Perf.	0.0043	Intact	210	375	32 100	Regular	
9002-3				Perf.	0.0042	Intact	220	390	30 900	Regular	
9002-4				Perf.	0.0040	Intact	225	410	29 300	Regular	
9008-1	5	5	0	0.0016	0.0030	Intact	440	725	16 600		Below velocity limit.
9009-1	8	8	2	0.0022	0.00385	Intact	210	340	35 400		
9009-2				Perf.	0.0042	Intact	260	420	28 600	Regular	
9009-3				Perf.	0.0036	Intact	325	530	22 700	Barely perforated	
9009-4				0.0018	0.0035	Intact	370	610	19 700		
9013-1	11	11	6	Perf.	0.0045	Intact	200	325	37 000	Regular	
9013-2				Perf.	0.0044	Intact	215	355	33 900	Regular	
9013-3				Perf.	0.0044	Intact	240	390	30 900	Regular	
9013-4				Perf.	0.0043	Intact	260	420	28 600	Regular	
9013-5				Perf.	0.00365	Intact	270	440	27 300	Regular	
9013-6				Perf.	0.0034	Intact	275	445	27 000	Barely perforated	

TABLE B-I. (Continued)

Target material: 0.002-in. single sheet beryllium-copper (half-hard)
Projectile: 0.00202-in.-diameter borosilicate spheres

1	2	3	4	5	6	7	8	9	10	11	12
9000-1	4	4	2	Perf.	0.0047	Intact	180	290	21 500	Regular	Above velocity limit.
9001-1	19	19	2	Perf.	0.0043	Intact	195	315	38 000	Regular	
9001-2				0.0025	0.0036	Intact	240	390	30 900		
9001-3				Perf.	0.0042	Intact	245	405	29 700	Regular	
9001-4				0.00225	0.0036	Intact	295	480	25 000		
9002-1	13	10	4	Perf.	0.0045	Intact	198	360	33 400	Regular	
9002-2				Perf.	0.0043	Intact	210	375	32 100	Regular	
9002-3				Perf.	0.0042	Intact	220	390	30 900	Regular	
9002-4				Perf.	0.0040	Intact	225	410	29 300	Regular	
9008-1	5	5	0	0.0016	0.0030	Intact	440	725	16 600		Below velocity limit.
9009-1	8	8	2	0.0022	0.00385	Intact	210	340	35 400		
9009-2				Perf.	0.0042	Intact	260	420	28 600	Regular	
9009-3				Perf.	0.0036	Intact	325	530	22 700	Barely perforated	
9009-4				0.0018	0.0035	Intact	370	610	19 700		
9013-1	11	11	6	Perf.	0.0045	Intact	200	325	37 000	Regular	
9013-2				Perf.	0.0044	Intact	215	355	33 900	Regular	
9013-3				Perf.	0.0044	Intact	240	390	30 900	Regular	
9013-4				Perf.	0.0043	Intact	260	420	28 600	Regular	
9013-5				Perf.	0.00365	Intact	270	440	27 300	Regular	
9013-6				Perf.	0.0034	Intact	275	445	27 000	Barely perforated	

TABLE B-I. (Continued)

Target material: 0.0015-in. Pegasus detector
Projectile: 0.00013-in.-diameter borosilicate spheres

1	2	3	4	5	6	7	8	9	10	11	12
9226-1	2	2	0	0.0022	0.00385	Intact	198	330	36 500		Spurious signal on projectile monitor.
9231-1	5	3	0	0.0018	0.0035		275	445	27 000		
9234-1	6	6	0	0.0020	0.00375		200	305	39 400		10 microseconds offset on projectile monitor. This point below velocity limit.
9234-2				0.0015	0.0028		365	605	19 800		
9239-1	9	9	1	Perf.	0.0039		245	400	30 100	Regular	
9241-1	12	11	0	0.0019	0.0033		320	520	23 100		
9243-1	17	17	0	0.0024	0.00385		210	340	35 400		
9243-2				0.00195	0.0038		225	365	33 000		
9243-3				0.0019	0.0032		230	370	32 500		
9243-4				0.00185	0.0031		235	380	31 600		
9245-1	16	11		Perf.	0.0039		225	365	33 000	Regular	
9245-2				0.00215	0.0039		235	370	32 500		
9245-3				0.0020	0.0036		242	380	31 600		
9251-1	15	12	0	0.0025	0.0043		180	285	42 200		This point above velocity limit. 20 microsecond offset on impact flash.
9251-2				0.00225	0.00415		185	290	41 500		
9256-1	11	11	0	0.0027	0.0039		190	305	39 400		
9256-2				0.0021	0.00355		195	315	38 200		
9306-1	4	4	1	0.0021	0.0035	Intact	195	318	37 700		
9306-2				0.0019	0.0034		210	340	35 400		
9306-3				Perf.	0.0036		215	345	34 900		

TABLE B-I. (Concluded)

Target material: 0.0015-in. Pegasus detector
Projectile: 0.00202-in.-diameter borosilicate spheres

1	2	3	4	5	6	7	8	9	10	11	12
9022-1	12	10	0	0.0034	0.0048	Intact	545	905	13 300		
9022-2				0.0031	0.0047	Intact	600	990	12 100		
9025-1	29	29	4	Perf.	0.0054	Intact	340	555	21 700	Regular	Above velocity limit.
9025-2				0.0024	0.0042	Intact	555	900	13 300		
9025-3				Perf.	0.0042	Intact	595	975	12 300	Tear	
9025-4				0.0015	0.0035	Intact	695	1120	9 900		Below velocity limit.
9034-1	4	2	0	0.0027	0.00405	Intact	600	1000	12 200		
9036-1	6	6	0	0.00255	0.0041	Intact	510	830	14 400		
9050-1	7	6	1	Perf.	0.0042	Intact	550	850	14 100	Tear	
9068-1	10	10	2	0.0020	0.00385	Intact	455	745	16 100		All perforations above velocity limit.
9083-1	18	18	3	Perf.	0.0038	Intact	460	770	15 600	Tear	Two perforations above velocity limit; therefore not recorded.
9083-2				0.0021	0.0033	Intact	520	860	14 000		
9083-3				0.0021	0.0028	Intact	530	880	13 700		
9083-4				0.00165	0.00345	Intact	545	905	13 300		
9095-1	11	9	1	Perf.	0.0050	Intact	385	660	18 200	Barely perforated	
9095-2				0.0026	0.0037	Intact	505	830	14 400		
9095-3				0.00175	0.0031	Intact	522	860	14 000		
9096-1	8	8	1	Perf.	0.0046	Intact	358	690	17 400	Tear	
9096-2				0.0020	0.0048	Intact	440	735	16 400		
9096-3				0.0016	0.0036	Intact	497	820	14 600		

APPENDIX C

SUMMARY OF CALIBRATION TESTS AT HAYES INTERNATIONAL

Target	Projectile Diameter (μ)	Date Fired	Shot No.	Velocity 1000 fps	Perforation Diameter (μ)	Crater Diameter (μ)	Remarks
0.016-in. Pegasus Panels	436 ±20	10/4/66	3	14.1	871		No Mylar damage
			8	16.6	966		Mylar damage
				16.6	964		Mylar damage
				16.6	910		Mylar damage
			9	15.1	951		Mylar damage
			12	19.3	1005		Mylar perforation
			13	16.5	930		Mylar damage
		10/5/66	6	15.1	922		Mylar damage
			9	18.1	942		Mylar perforation
	367 ±10	10/6/66	5	16.0		709	Deep crater
			6	16.5		791	Almost perforated
			8	18.5	847		No Mylar damage
			11	14.0		760	Deep crater
		10/7/66	2	15.3		760	Deep crater
		10/10/66	6	14.3		733	Deep crater
			9	18.5	825		No Mylar damage
				18.5	779		No Mylar damage
	309 ±14	10/5/66	12	17.0		711	Deep crater
			13	17.0		697	Deep crater
				17.7		706	Deep crater
				18.7		726	Deep crater
0.008-in. Pegasus Panels	309 ±14	10/19/66	4	14.1	621		Mylar perforation
			6	17.5	665		Mylar perforation
				16.0	633		Mylar perforation
	249 ±10	10/25/66	3	15.2	498		Mylar damage
				15.2	502		Mylar damage
				15.3	527		Mylar damage
				15.4	536		Mylar perforation
				15.5	551		Mylar perforation
				15.5	553		Mylar perforation
			4	14.8	561		Mylar perforation
				14.8	573		Mylar perforation
			7	16.7	512		Mylar damage
			8	14.5	524		Mylar perforation
			12	16.1	515		Mylar damage
		10/31/66	2	16.2	449		Mylar damage
				16.2	500		Mylar damage
				16.2	541		Mylar perforation
			3	13.4		517	Deep crater

Target	Projectile Diameter (μ)	Date Fired	Shot No.	Velocity 1000 fps	Perforation Diameter (μ)	Crater Diameter (μ)	Remarks
0.008-in. Pegasus Panels (Cont'd)	249 ±10 (Cont'd)	11/1/66	1	14.1	529		Mylar perforation
				14.1	485		Mylar perforation
				14.1	478		Mylar perforation
				14.1	478		Mylar perforation
				14.1	475		Mylar perforation
				14.1		515	Deep crater
				14.1		498	Deep crater
				14.1		475	Deep crater
				14.1		473	Deep crater
				14.1		471	Deep crater
			2	15.2	551		Mylar perforation
	216 ±15	11/1/66	3	15.6		478	Deep crater
				15.6		454	Shallow crater
				15.6		454	Shallow crater
				15.6		447	Shallow crater
			6	16.2	471		Mylar perforation
				16.2	459		Mylar damage
			7	15.5		405	Deep crater
			9	16.6	456		Mylar damage
				16.6		454	Deep crater
				16.6		451	Deep crater
			12	14.6		430	Shallow crater
			13	15.1		473	Deep crater
				15.1		425	Deep crater
				15.1		413	Shallow crater
		11/2/66	3	21.3	485		Mylar damage
				21.3	471		Mylar damage
				21.3	471		Mylar damage
				21.3	459		Mylar damage
				21.3	451		Mylar damage
			4	17.7	468		Mylar perforation
		11/3/66	5	15.1		454	Deep crater
				15.1		444	Deep crater
				15.1		442	Deep crater
				15.1		437	Deep crater
				15.1		425	Deep crater
			7	13.8		454	Shallow crater
				13.8		454	Shallow crater
				13.8		417	Shallow crater
		11/4/66	2	17.0	485		Mylar perforation
0.0015-in. Pegasus	133 ±9	1/31/67	2	15.5	279		Position No. 2
			7	15.6	277		Position No. 2
		2/9/67	3	9.3	294		Position No. 3
				9.5		308	Position No. 4
			5	13.0	294		Position No. 3
					304		

Target	Projectile Diameter (μ)	Date Fired	Shot No.	Velocity 1000 fps	Perforation Diameter (μ)	Crater Diameter (μ)	Remarks
0.0015-in. Pegasus (Cont'd)	$70.4^{+2.2}_{-3.7}$	12/30/66	5	12.8	184		Position No. 4
			7	19.4	201		Position No. 4
		1/9/67	2	16.6	191		Position No. 1
		1/10/67	1	16.0	186		Position No. 5
			2	16.6	199		Position No. 4
					196		
				15.3	190		Position No. 5
					193		
					191		
			3	14.1	173		Position No. 1
					186		
					182		
				15.2	175		Position No. 2
					185		
					176		
					174		
					182		
		1/13/67	2	16.6	203	201	Position No. 1
						192	
				16.1	172	182	Position No. 2
					192	188	
					191		
					195		
					196		
					182		
				18.0	198		Position No. 4
					179		
					183		
			4	14.2		193	Position No. 1
				14.0	189		Position No. 3
					197		
					175		
					191		
				13.8		202	Position No. 4
		1/16/67	4	14.4	184		Position No. 1
					186		
				14.4	181		Position No. 2
				14.2	180	192	Position No. 3
						188	
						197	

Target	Projectile Diameter (μ)	Date Fired	Shot No.	Velocity 1000 fps	Perforation Diameter (μ)	Crater Diameter (μ)	Remarks
0.0015-in. Pegasus (Cont'd)	$70.4^{+2.2}_{-3.7}$ (Cont'd)	1/17/67	1	14.5	202	198	Position No. 1
					179		
					174		
					185		
				14.5	180		Position No. 2
					179		
					175		
				14.3	188	188	Position No. 4
					192	193	
					182		
					191		
					176		
					177		
					177		
			2	15.5	178		Position No. 2
					180		
					193		
					202		
				15.1	188		Position No. 3
					202		
			3	16.7	197	204	Position No. 2
					194	176	
					197	(8 more)	
					207		
					201		
					(30 more)		
				16.6	199	196	Position No. 3
					191		
				16.5	191	203	Position No. 4
					201		
			4	12.8	197	202	Position No. 3
				12.8	191		Position No. 4
		1/23/67	2	13.8	176		Position No. 2
		1/24/67	1	14.8	190	194	Position No. 2
					185	(1 more)	
					(8 more)		
				14.8	181	190	Position No. 3
					188	186	
					186	(3 more)	
					(1 more)		
				14.8	196	187	Position No. 4
						195	
		1/26/67	2	14.6	194	200	Position No. 2

Target	Projectile Diameter (μ)	Date Fired	Shot No.	Velocity 1000 fps	Perforation Diameter (μ)	Crater Diameter (μ)	Remarks
0.001-in. Stainless Steel (302)	216 ±15	11/21/66	1	16.2	390		Position No. 4
					384		
					377		
					380		
	133 ±9	2/9/67	1	10.4	191		Position No. 2
					176		
					178		
					180		
					173		
					187		
			4	18.7	176		Position No. 2
	$70.4^{+2.2}_{-3.7}$	12/21/66	2	16.7	111		Position No. 4
			4	18.8	117		Position No. 2
			5	18.0	124		Position No. 2
					133		
		12/22/66	3	13.5	116		Position No. 4
		12/27/66	3	17.8	134		Position No. 4
		1/13/67	2	17.2	124		Position No. 2
					126		
					128		
					127		
			4	21.6	123		Position No. 4
					128		
		1/17/67	1	14.5	120		Position No. 4
			2	16.2	126		Position No. 4
					118		
			4	13.7	119		Position No. 4
		1/20/67	3	16.6	107		Position No. 4
		1/23/67	3	13.7	113		Position No. 4
		2/8/67	3	14.9	113		Position No. 1
				14.7	106		Position No. 2
					106		
		2/9/67	4	18.7	107		Position No. 2
	$57.7^{+3.1}_{-2.6}$	1/25/67	5	15.2	96		Position No. 2
					97		
				15.2	99		Position No. 4

Target	Projectile Diameter (μ)	Date Fired	Shot No.	Velocity 1000 fps	Perforation Diameter (μ)	Crater Diameter (μ)	Remarks
0.001-in. Stainless Steel (302) (Cont'd)	$42.2^{+2.3}_{-4.1}$	1/20/67	2	14.7		68 65 67 69 (4 more)	Position No. 4
		1/31/67	1	13.1	195		Position No. 4
			2	15.2	208		Position No. 4
			4	14.7	217 218 201		Position No. 1
		2/9/67	5	13.0	194 204		Position No. 1-R
		2/10/67	2	15.2	187 201		Position No. 1-R
				15.2	203 188		Position No. 2-R
				15.0	191		Position No. 3-R
0.002-in. Stainless Steel (302)	$70.4^{+2.2}_{-3.7}$	1/16/67	4	13.4		122 115 114 114	Position No. 1
		1/17/67	4	11.9		130 131	Position No. 1
				13.3		119 126	Position No. 3
		2/9/67	3	9.4		118 123	Position No. 1-R
				9.4		121	Position No. 2-R
			4	18.3		125 128	Position No. 1-R
				18.3		130	Position No. 2-R
		2/10/67	5	10.4		131 130	Position No. 1-R
				10.4		125 127 121 128 122 125 129 128	Position No. 2-R
				10.4		132	Position No. 3-R
	$57.7^{+3.1}_{-2.6}$	1/31/67	1	13.1		101 94 93 92	Position No. 4

APPENDIX D

SUMMARY OF CALIBRATION TESTS AT ILLINOIS INSTITUTE OF TECHNOLOGY RESEARCH INSTITUTE

Item	Round Number	Sphere Diam (μ)	Target Material	Target Thickness (Mils)	Sabot Velocity (fps)	Sphere Velocity (fps)	Hole Diam (μ)	Crater Diam (μ)
1	48	48.6	Stainless Steel	2	21 100	No Data	143 143 143 135 127 127 112	
1	60	48.6	Stainless Steel	2	22 000[a]	21 500[a]	159 143 143 112 112 96	
1	61	48.6	Stainless Steel	2	22 000[a]	21 000[a]	143 127	
2	52	48.6	Pegasus	1.5	20 600	5.577	127 80	
2	54	48.6	Pegasus	1.5	No Data	No Data	302 286	
2	55	48.6	Pegasus	1.5	18 000[a]	No Data	222 222 191 159	
2	56	48.6	Pegasus	1.5	16 000[a]	No Data	334 238 238 159	
2	57	48.6	Pegasus	1.5	11 500[a]	No Data	No Clean Circular Penetration	286 143
2	58	48.6	Pegasus	1.5	13 700[a]	No Data	286	127 112

Item	Round Number	Sphere Diam (μ)	Target Material	Target Thickness (Mils)	Sabot Velocity (fps)	Sphere Velocity (fps)	Hole Diam (μ)	Crater Diam (μ)
3	43	48.6	Stainless Steel	1.0	21 000	6.035	143 143	
3	49	48.6	Stainless Steel	1.0	19 400	5.898	143 143 127 127 127 112 112 96 96 88	
3	59	48.6	Stainless Steel	1.0	18 200[a]	15 000[a]	159	(Does not look like ball impact.)
4	36	38.6	Stainless Steel	1.0	21 500	19 800	143	
5	26	20	Stainless Steel	1.0	22 000[a]	(Irregular shaped, no circular holes - possible conglomerate impacts.)		
5	27	20	Stainless Steel	1.0	22 500	(Irregular shaped, no circular holes - possible conglomerate impacts.)		
6	130	45	Pegasus	8.0	21 700	No Data	445 430	
7	260	42	Pegasus	16.0	21 900	20 950	715	
7	240	29	2024T4	16.0	19 000	No Data		396 350 315 254 239 222

a. Velocity not verified with image converter data.

APPENDIX E

SUMMARY OF CALIBRATION TESTS AT SPACE SCIENCES LABORATORY, MSFC

Target	Projectile	Velocity km/sec	P — Penetration NP — Nonpenetration	Firing Reference No.
0.0406-cm Pegasus Panels	210-micron sodium-lime beads (ρ = 2.6 g/cm^3)[a] (m = 1.25 × 10^{-5}g)	6.99	P	C-2-068
		5.94	P	C-2-069
		5.56	P	C-2-073
		5.43	NP	C-2-075
		4.12	NP	C-2-074
	177-micron sodium-lime beads (ρ = 2.5 g/cm^3)[a] (m = 0.72 × 10^{-5}g)	7.16	P	D-2-001
		6.79	P	C-2-076
		6.79	P	D-2-006
		6.65	P	D-2-003
		6.45	P	D-2-007
		6.39	P	D-2-002
		6.21	NP	D-2-005
		6.08	NP	D-2-008
	149-micron sodium-lime beads (ρ = 2.5 g/cm^3)[a] (m = 0.42 × 10^{-5} gm)	7.32	P	020
		7.24	P	009
		7.12	P	021
		7.08	NP	019
		6.78	NP	022
		6.52	NP	024
		6.03	NP	010
		5.80	NP	004

a. In some cases there are bubbles in the glass that will lower the density of individual beads. However, an additional check was made by this laboratory which indicated that the beads do have an average density of 2.4755 g/cm^3 .

REFERENCES

1. Scully, C. N.: Experimental Hypervelocity Impact Research. Final Report NAS8-21007, SID 67-251; also Final Report NAS8-21115, SID 67-1209, North American Rockwell, Downey, Calif.

2. Hull, W. C.; Fleming, F. W.; Scott, J. L.; and Smith, L. R.: Experimental Hypervelocity Impact Research. NAS8-20345, Hayes International Corp., Birmingham, Ala., March 2, 1967.

3. Hull, W. C.; Fleming, F. W.; Scott, J. L.; and Smith, L. R.: Experimental Hypervelocity Impact Research. NAS8-20345, Hayes International Corp., Birmingham, Ala., March 15, 1968.

4. Jeslis, J.: Experimental Hypervelocity Impact Research Program. Final Report NAS8-20337, Illinois Institute of Technology Research Institute, May 1968.

5. Fish, R. H.; and Summers, J. L.: The Effects of Material Properties on Threshold Penetration. Proceedings of 7th Hypervelocity Impact Symposium, February 1965.

NASA-Langley, 1969 —— 14 M430

NATIONAL AERONAUTICS AND SPACE ADMINISTRATION
WASHINGTON, D.C. 20546

OFFICIAL BUSINESS

FIRST CLASS MAIL

POSTAGE AND FEES PAID
NATIONAL AERONAUTICS AND
ADMINISTRATION

17U 001 39 51 3DS 69226 0C9C3
AIR FORCE WEAPONS LABORATORY/AFWL/
KIRTLAND AIR FORCE BASE, NEW MEXICO 8711

ATT E. LOU BOWMAN, ACTING CHIEF TECH. LI

POSTMASTER: If Undeliverable (Section 158 Postal Manual) Do Not Return

"The aeronautical and space activities of the United States shall be conducted so as to contribute . . . to the expansion of human knowledge of phenomena in the atmosphere and space. The Administration shall provide for the widest practicable and appropriate dissemination of information concerning its activities and the results thereof."

—NATIONAL AERONAUTICS AND SPACE ACT OF 1958

NASA SCIENTIFIC AND TECHNICAL PUBLICATIONS

TECHNICAL REPORTS: Scientific and technical information considered important, complete, and a lasting contribution to existing knowledge.

TECHNICAL NOTES: Information less broad in scope but nevertheless of importance as a contribution to existing knowledge.

TECHNICAL MEMORANDUMS: Information receiving limited distribution because of preliminary data, security classification, or other reasons.

CONTRACTOR REPORTS: Scientific and technical information generated under a NASA contract or grant and considered an important contribution to existing knowledge.

TECHNICAL TRANSLATIONS: Information published in a foreign language considered to merit NASA distribution in English.

SPECIAL PUBLICATIONS: Information derived from or of value to NASA activities. Publications include conference proceedings, monographs, data compilations, handbooks, sourcebooks, and special bibliographies.

TECHNOLOGY UTILIZATION PUBLICATIONS: Information on technology used by NASA that may be of particular interest in commercial and other non-aerospace applications. Publications include Tech Briefs, Technology Utilization Reports and Notes, and Technology Surveys.

Details on the availability of these publications may be obtained from:

SCIENTIFIC AND TECHNICAL INFORMATION DIVISION

NATIONAL AERONAUTICS AND SPACE ADMINISTRATION

Washington, D.C. 20546